OPEN ACCESS
Saudi Journal of Civil Engineering
Abbreviated Key Title: Saudi J Civ Eng
ISSN 2523-2657 (Print) |ISSN 2523-2231 (Online)
Scholars Middle East Publishers, Dubai, United Arab Emirates
Journal homepage: https://saudijournals.com

Review Article

Effect of in-plane Statically Applied Normal Loads on Nonlinear Fundamental Frequency of Thin Rectangular SCSC Plate

P. D. Onodagu[1*], B. O. Adinna[1] and V. O. Okonkwo[1]

[1]Department of Civil Engineering, Nnamdi Azikiwe University, P. M. B. 5025, Awka, Nigeria

DOI: 10.36348/sjce.2021.v05i02.004 | **Received:** 10.02.2021 | **Accepted:** 22.02.2021 | **Published:** 18.03.2021

***Corresponding author:** P. D. Onodagu

Abstract

This paper determines analytically the effect of in-plane statically applied normal loads on nonlinear fundamental frequency of thin rectangular plate with edge constraints as simply supported – clamped – simply supported – clamped (SCSC). The weak-form variational principle was used to formulate the energy functional of the plate problems. Algebraic polynomial displacements were used as shape functions. Both linear and nonlinear buckling loads were numerically computed at various aspect ratios. The nonlinear fundamental frequencies were computed at various aspect ratios by considering the presence of in-plane applied normal loads and also by considering the absence of in-plane loads. Furthermore, the variations in the ratios of nonlinear to linear buckling loads; and nonlinear fundamental to natural nonlinear fundamental frequencies were determined at various aspect ratios. The numerical value of linear buckling load obtained for a square plate was compared with results from previous works found in literature, and there was satisfactory convergence with percentage error of 4.90. Conclusively from the analytical and numerical results obtained, in-plane statically applied normal loads affect the nonlinear fundamental frequency of thin rectangular SCSC plate.

Keywords: Algebraic polynomial, shape function, buckling load, linear, nonlinear, weak-form, variational principle, fundamental frequency.

INTRODUCTION

The high demands for weight economy in the applications of flat thin plates in marine, naval and vehicular industries have been continually on the rise for the purposes of attaining full optimization [1, 2]. Flat rectangular plates are structural elements that are more often subjected to either in-plane loadings or out-of-plane loadings or both. These loads can be either static or dynamic or both.

The application of flat thin rectangular plates to sustain in-plane loadings has created wide research fields based on the mode of deformations and on the characteristic responses to such loadings. Buckling is the characteristic mode of deformation of flat rectangular plate due to in-plane loading. Buckling is a phenomenon in which the structural element performs an infinitesimal deformation in the direction of its largest dimension, which is a process by which the structural element adjusts itself to a new equilibrium position. However, contrary to the mode of responses of other structural elements when subjected to in-plane loadings, flat thin rectangular plates exhibit double buckling modes of responses, from which the stakeholders on the applications of thin rectangular plates seek to utilize in their designs to achieve stability and weight efficiency.

Flat thin rectangular plates have the capacity to respond linearly to in-plane loadings up to bifurcation points without any appreciable loss to equilibrium conditions [3]. Within this regime, there is infinitesimal shift in the initial configuration of the plate with respect to the direction of largest dimension, which is linear in nature. This deformation is classified as first buckling or simply buckling; and the resulting load is called the buckling load. Therefore the analysis within this regime is linear.

Moreover, flat thin rectangular plates have the ability to sustain additional in-plane loads of magnitudes several integers times the buckling loads before reaching the second buckling, otherwise known as the post buckling, after which the plates may lose

their stability conditions. At this stage, the plates experience finite deflections in the directions of the largest dimensions. Thus the analysis has to shift from linear to nonlinear condition.

The determination and evaluation of the conditions associated with the post buckling phenomenon as well as the corresponding methods of analysis, all form the cruxes of the researches on the applications of flat plates in marine, naval and vehicular structures. Different approximation techniques have been used to determine the buckling and post buckling behaviour of thin rectangular plates [4-7].

The primary objective of this work is to determine the effect of statically applied normal in-plane loading on the nonlinear fundamental frequency of simply supported – clamped – simply supported - clamped (SCSC) thin rectangular plate. The secondary objective is to use Weak-form variational method to calculate the eignvalues or the buckling and nonlinear buckling loads respectively. The efficacy and the degree of convergence of weak-form variational method have not been adequately exploited in the study of buckling and post buckling behaviour of rectangular plates. Furthermore, the third objective of this work is to use algebraic polynomial shape functions that simulate the deflection function and satisfy the geometric boundary conditions of SCSC rectangular plate as alternative to trigonometric shape functions.

Related works

The desire to achieve weight efficiency in the applications of thin rectangular plates in the construction of aircrafts, ship and marine vessels, road and railway vehicular structures has created a lot of research interests in the analysis of thin rectangular plates; and sequel to such developments, many research works have been done on the buckling and post buckling analyses of thin rectangular plates. For instance, a sponsored research work on the post buckling behaviour of structures by North Atlantic Treaty Organization (NATO) was carried out [8]. However, different researchers employed different analytical and numerical techniques to investigate the behaviour of thin rectangular plates under buckling and post buckling conditions [9]. Investigated the buckling and vibration of stiffened panels or single plates with clamped ends by using Lagrangian multipliers to couple sinusoidal modes of the plates and then VICNOPT computer program to calculate the eignvalues. The dynamic stability of composite skew plates subjected to periodic in-plane load was studied using finite element approach [10]. Also [11, 12], studied the dynamic stability of all clamped and simply supported edges respectively of thin rectangular plates subjected to in-plane loadings using energy methods. Some aspects of dynamic buckling of plates under in-plane pulse loading were investigated by [13] using finite element computer code ANSYS 8.1. Furthermore, the effect of in-plane forces on frequency parameters was studied on stiffened plates using finite element method [14]; whereas [15] employed an improved moving least square Ritz method on similar conditions. Also, [16] studied the effects of in-plane loading on vibration of composite plates using the finite element method. Buckling of generally orthotropic rectangular plate under compound in-plane linearly bending-compressive loading was studied by [17] using Ritz method. Also, [18] used boundary element method based meshless solution to study buckling and vibration problems of orthotropic plates. The critical buckling load of rectangular plate was evaluated using integrated force method [19]. Moreover, [20] studied the buckling behavior of rectangular plates having linearly varying in-plane loading on two opposite simply supported edges. However [21], employed ANSYS to study the buckling behaviour of laminated composite plates subjected to in-plane loading. Whereas [22] extended the studies to shells and solid models of homogenous and functionally graded plates. The buckling and post buckling load characteristics of all clamped edges thin rectangular plates using a combination of direct integration and work principle were studied [23, 24]. Moreover, the buckling behaviour of composite plates with initial imperfection was studied by [25] using finite element method [26], employed asymptotical and non-stationary finite element methods to investigate different aspects of static and dynamic response of post buckled thin plates. A study of large amplitude free vibrations of thin plates was done using finite element formulations for arbitrary shapes [27]. Also, [28] developed a simple formula for such studies to determine the first free mode of vibration of beams and plates.

Theoretical Formulations

Fig. 1 shows a plan view of a thin, isotropic rectangular plate, which has its edge constraint conditions as simply-supported (S), clamped ©, simply-supported (S) and clamped ©, otherwise referred to as SCSC rectangular plate.

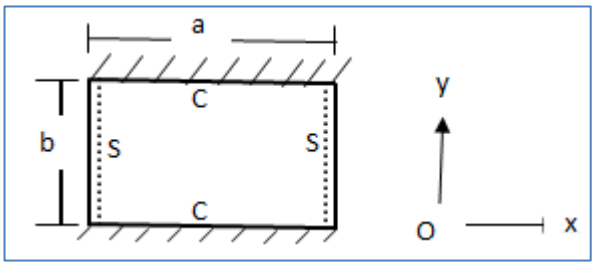

Fig-1: A plan view of thin isotropic SCSC rectangular plate

The plate's characteristic dimensions are defined by *a* and *b* as the length and width respectively. The plate is assumed to be flat and invariant in its engineering properties of Young modulus, *E* and Poisson's ratio, μ; and it has constant mass density, ρ.

However, the plate is subjected to compressively unidirectional loading in x-direction as shown in Fig. 2. In this work, most of the fundamental hypotheses for nonlinear thin plate theory are adopted. Here it is assumed that the plate is capable of carrying loads beyond the bifurcation point; and it is physically assumed that the in-plane stiffness of the plate is very high compared with the lateral stiffness of the plate so that second-order effects dominate the plate's deformation response; and that the plate is expected to buckle in the pattern of stable equilibrium path. Therefore, in this work, it is assumed that the deformation caused by the compressive loads is large compared to the plate's thickness, *h* so that the plate analysis is shifted from rigid (linear) to flexible (nonlinear) plate analysis.

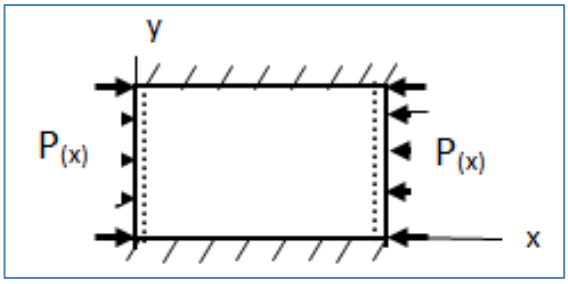

Fig-2: A rectangular SCSC plate under compressively unidirectional in-plane loading

Thus, the governing nonlinear differential equilibrium equations that simulated that of the Von Karman's thin plate differential equilibrium equations are sufficed and are stated accordingly [29, 30]:

$$\nabla^4 w = \frac{1}{D}\left[q + \frac{\partial^2 F}{\partial y^2}\frac{\partial^2 w}{\partial x^2} - 2\frac{\partial^2 F}{\partial x \partial y}\frac{\partial^2 w}{\partial x \partial y} + \frac{\partial^2 F}{\partial x^2}\frac{\partial^2 w}{\partial y^2} - \rho h \ddot{w}\right] \quad (1)$$

$$\nabla^4 F = Eh\left[\left(\frac{\partial^2 w}{\partial x \partial y}\right)^2 - \frac{\partial^2 w}{\partial x^2}\frac{\partial^2 w}{\partial y^2}\right] \quad (2)$$

Where
w = lateral deflection
q = lateral load on plate's surface
F = Airy's stress function
h = thickness of the plate
$\ddot{w}$ = second derivative of w with respect to time, t.
D = rigidity of the plate, defined as given in (3).

$$D = \frac{Eh^3}{12(1-\mu^2)} \quad (3)$$

Development of Functional of the Plate Problem

The weak-form variational principle is adopted to formulate the functional of the plate problem. Let the weighting function be defined as *V(x,y);* and the variational statement of the plate problem is then given using Eq. (1) as:

$$0 = \int_0^a \int_0^b V(x,y)\left[\frac{\partial^4 w}{\partial x^4} + 2\frac{\partial^4 w}{\partial x^2 \partial y^2} + \frac{\partial^4 w}{\partial y^4} - K\left(q + \frac{\partial^2 F}{\partial y^2}\frac{\partial^2 w}{\partial x^2} - 2\frac{\partial^2 F}{\partial x \partial y}\frac{\partial^2 w}{\partial x \partial y} + \frac{\partial^2 F}{\partial x^2}\frac{\partial^2 w}{\partial y^2} - \rho h \ddot{w}\right)\right] dxdy \quad (4)$$

Where

$$K = \frac{1}{D} \quad (5)$$

Subsequently integration by parts is performed on Eq. (4) to trade derivatives from *w* and *F* to *V(x,y)*. The resulting integration is as expressed in Eq. (6):

$$\begin{aligned} 0 = \int_0^a \int_0^b & \left[\frac{\partial^2 V}{\partial x^2}\frac{\partial^2 w}{\partial x^2} + 2\frac{\partial^2 V}{\partial x \partial y}\frac{\partial^2 w}{\partial x \partial y} + \frac{\partial^2 V}{\partial y^2}\frac{\partial^2 w}{\partial y^2} \pm 2KF\frac{\partial^2 V}{\partial x \partial y}\frac{\partial^2 w}{\partial x \partial y} \pm KF\frac{\partial^2 V}{\partial y^2}\frac{\partial^2 w}{\partial x^2} \pm KF\frac{\partial^2 V}{\partial x^2}\frac{\partial^2 w}{\partial y^2} - KVq + KV\rho t\ddot{w}\right] dxdy \\ & + \int_0^a \left\{\left[2\frac{\partial V}{\partial x}(M_{xy}) - V\left(\frac{\partial M_y}{\partial y}\right) + \frac{\partial V}{\partial y}(M_y) + 2KF\frac{\partial V}{\partial x}(M_{xy}) + KV\frac{\partial F}{\partial y}(M_x) + 2KVF\left(\frac{\partial M_{xy}}{\partial x}\right) - KF\frac{\partial V}{\partial y}(M_x)\right]_0^b\right\} dx \\ & + \int_0^b \left\{\left[-V\left(\frac{\partial M_x}{\partial x}\right) + \frac{\partial V}{\partial x}(M_x) - 2V\left(\frac{\partial M_{xy}}{\partial y}\right) - KF\frac{\partial V}{\partial y}(M_{xy}) - KVF\left(\frac{\partial M_{xy}}{\partial y}\right) - 2KV\frac{\partial F}{\partial y}(M_{xy}) - KF\frac{\partial V}{\partial x}(M_y)\right.\right. \\ & \left.\left. + KV\frac{\partial F}{\partial x}(M_y)\right]_0^a\right\} dy \end{aligned} \quad (6)$$

Where $V(x,y) = V$. The last two expressions in the curl brackets of the integrands of Eq. (6) are the yielded natural boundary conditions, and each of them is identically satisfied at the boundary of the plate. Consequent upon, they are dropped in the further analysis of this work. The first expression in Eq. (6), which is contained in square bracket is the yielded functional of the plate problem, and it is also identically satisfied. For simplicity, it is assumed that the plate vibrates harmonically and performs sinusoidal time response, and then the inertia term in Eq. (6) is expressed as given in Eq. (7):

$$\rho h\ddot{w} = -\rho h\omega^2 w(x,y) \tag{7}$$

Where ω = cyclic natural frequency.

Substitution of Eq. (7) into Eq. (6) yields Eq. (8).

$$0 = \int_0^a \int_0^b \left[\frac{\partial^2 V}{\partial x^2}\frac{\partial^2 w}{\partial x^2} + 2\frac{\partial^2 V}{\partial x \partial y}\frac{\partial^2 w}{\partial x \partial y} + \frac{\partial^2 V}{\partial y^2}\frac{\partial^2 w}{\partial y^2} + 2KF\frac{\partial^2 V}{\partial x \partial y}\frac{\partial^2 w}{\partial x \partial y} + KF\frac{\partial^2 V}{\partial y^2}\frac{\partial^2 w}{\partial x^2} + KF\frac{\partial^2 V}{\partial x^2}\frac{\partial^2 w}{\partial y^2} - KVq - \omega^2 MKVw\right] dxdy \tag{8}$$

Where

$$M = \rho * h \tag{9}$$

The functional of Eq. (8) is a generic energy functional for thin isotropic rectangular plates, formulated by using the weak-form variational method.

Polynomial Displacement Functions

The lateral displacement function for the plate is developed from the concept that the deflection of plate is equivalent to the deflections of orthogonal beam network. The polynomial functions which satisfy the deflection function for each of the beam running along each of the orthogonal direction and which also satisfy the geometric boundary conditions are determined. Thus for x-direction, the polynomial functions that satisfy the beam deflection as well as the geometric boundary conditions at first mode are:

$$w(x) = A_1\left[\left(\frac{x}{a}\right) - 2\left(\frac{x}{a}\right)^3 + \left(\frac{x}{a}\right)^4\right] \tag{10}$$

Similarly for y-direction, the functions are as follows:

$$w(y) = A_2\left[\left(\frac{y}{b}\right)^2 - 2\left(\frac{y}{b}\right)^3 + \left(\frac{y}{b}\right)^4\right] \tag{11}$$

Therefore the plate deflection is given as in Eq. (12).

$$w(x,y) = A_{12}\left[\left(\frac{x}{a}\right) - 2\left(\frac{x}{a}\right)^3 + \left(\frac{x}{a}\right)^4\right]\left[\left(\frac{y}{b}\right)^2 - 2\left(\frac{y}{b}\right)^3 + \left(\frac{y}{b}\right)^4\right] \tag{12}$$

Where A_{12} is undetermined coefficient known as the amplitude of deflection, and it is defined as:

$$A_{12} = A_1 * A_2 \tag{13}$$

Stress Function

The expression for stress function for SCSC rectangular plate is determined by performing successive integration on the Von Karman's differential compatibility equation of Eq. (2). By substituting Eq. (12) into Eq. (2) and performing successive integration, the expression for stress function F_{11} due to large deflection is given as in Eq. (14).

$$\begin{aligned} F_{11} = \frac{Qx^4y^6A_{12}^2}{3175200a^8b^8}\{&6a^3x^3(14b^4 - 15b^2y^2 + 10by^3 - 2y^4) - 42a^4x^2(14b^4 - 24b^3y + 21b^2y^2 - 10by^3 + 2y^4) \\ &+ 36a^2x^4(14b^4 - 30b^3y + 30b^2y^2 - 15by^3 + 3y^4) + 105a^6(14b^4 - 36b^3y + 39b^2y^2 - 20by^3 + 4y^4) \\ &- 5ax^5(70b^4 - 144b^3y + 141b^2y^2 - 70by^3 + 14y^4) \\ &+ x^6(70b^4 - 144b^3y + 141b^2y^2 - 70by^3 + 14y^4)\} \end{aligned} \tag{14}$$

However, the expression for stress function that includes the influence of axially compressive load is as given in Eq. (15).

$$\begin{aligned} F_{12} = \frac{Qx^4y^6A_{12}^2}{3175200a^8b^8}\{&6a^3x^3(14b^4 - 15b^2y^2 + 10by^3 - 2y^4) - 42a^4x^2(14b^4 - 24b^3y + 21b^2y^2 - 10by^3 + 2y^4) \\ &+ 36a^2x^4(14b^4 - 30b^3y + 30b^2y^2 - 15by^3 + 3y^4) + 105a^6(14b^4 - 36b^3y + 39b^2y^2 - 20by^3 + 4y^4) \\ &- 5ax^5(70b^4 - 144b^3y + 141b^2y^2 - 70by^3 + 14y^4) + x^6(70b^4 - 144b^3y + 141b^2y^2 - 70by^3 + 14y^4)\} \\ &- \frac{Py^2}{2} \end{aligned} \tag{15}$$

Amplitude of Deflection, A_{12}

The amplitude of deflection is a function of the rigidity characteristics of the rectangular plate under large deflection, and it is related to the lateral loads on the plate and to the rigidity of the constraints at the edges of the plate. For large deflection analysis, both the geometric and in-plane boundary conditions are considered. In this work, immovable edge conditions are assumed. Thus for SCSC rectangular plate, the general boundary conditions are [31, 32]:

$$u = v = w = w_o = N_{xy} = M_x = M_{xy} = \frac{\partial^2 w_o}{\partial x^2} = 0 \; at \; x = 0, a \tag{17}$$

$$u = v = w = w_o = \frac{\partial w}{\partial y} = \frac{\partial w_o}{\partial y} = 0 \; at \; y = 0, b \tag{18}$$

However, in this work, it is assumed that the uniform normal in-plane loads are applied in the x-direction only, which implies that $\frac{\partial^2 F}{\partial x^2} = \frac{\partial^2 F}{\partial x \partial y} = 0$. Thus the appropriate functional for SCSC rectangular plate under unidirectional normal in-plane loadings in x-direction is given as in Eq. (19).

$$0 = \int_0^a \int_0^b \left[\frac{\partial^2 V}{\partial x^2}\frac{\partial^2 w}{\partial x^2} + 2\frac{\partial^2 V}{\partial x \partial y}\frac{\partial^2 w}{\partial x \partial y} + \frac{\partial^2 V}{\partial y^2}\frac{\partial^2 w}{\partial y^2} + KF\frac{\partial^2 V}{\partial y^2}\frac{\partial^2 w}{\partial x^2} - KVq - \omega^2 MKVw \right] dxdy \tag{19}$$

To determine the amplitude of deflection, A_{12}, the inertia term of Eq. (19) is dropped so that Eq. (19) reduces to expression as given in Eq. (20).

$$\int_0^a \int_0^b \left[\frac{\partial^2 V}{\partial x^2}\frac{\partial^2 w}{\partial x^2} + 2\frac{\partial^2 V}{\partial x \partial y}\frac{\partial^2 w}{\partial x \partial y} + \frac{\partial^2 V}{\partial y^2}\frac{\partial^2 w}{\partial y^2} + KF\frac{\partial^2 V}{\partial y^2}\frac{\partial^2 w}{\partial x^2} \right] dxdy = \int_0^a \int_0^b KVq dxdy \tag{20}$$

In this work, the weighting function, *V(x,y)* is defined as given in Eq. (21).

$$V(x,y) = \left[\left(\frac{x}{a}\right) - 2\left(\frac{x}{a}\right)^3 + \left(\frac{x}{a}\right)^4 \right] \left[\left(\frac{y}{b}\right)^2 - 2\left(\frac{y}{b}\right)^3 + \left(\frac{y}{b}\right)^4 \right] \tag{21}$$

By substituting Eqs. (21), (14) and (12) into Eq. (20) and performing double integrations as required, and after simplifying yields Eq. (22).

$$(1.55446 * 10^{-9} a^4 b^4 KQ) A_{12}^3 + (0.0393651 a^4 + 0.0185034 a^2 b^2 + 0.00761905 b^4) A_{12} - 0.00666667 a^4 b^4 Kq = 0 \tag{22}$$

Let the aspect ratio, $\beta = \frac{a}{b}$, or $a = \beta b$ (23)

By solving Eq. (22) in terms of amplitude of deflection A_{12} yields a real root as expressed in Eq. (24).

$$A_{12} = \frac{-4.76533 * 10^8 b^4 \xi}{\left[Z_{1+}\sqrt{Z_2 + Z_3 \xi^3} \right]^{\frac{1}{3}}} + \zeta \left\{ 8.163212 * 10^{-5} \left[Z_{1+}\sqrt{Z_2 + Z_3 \xi^3} \right]^{\frac{1}{3}} \right\} \tag{24}$$

Where

$$\xi = (217\beta^4 + 102\beta^2 + 42) \tag{25}$$

$$Z_1 = 3.94211 * 10^{18} \beta^{12} b^{24} K^3 q Q^2 \tag{26}$$

$$Z_2 = 1.55403 * 10^{37} \beta^{24} b^{48} K^6 q^2 Q^4 \tag{27}$$

$$Z_3 = 1.98935 * 10^{38} \beta^{12} b^{24} K^3 Q^3 \tag{28}$$

$$\zeta = \frac{1}{\beta^4 b^8 KQ} \tag{29}$$

Nonlinear Fundamental Frequency

The nonlinear fundamental frequency is determined by invoking Eq. (19); and the lateral load term is dropped as expressed in Eq. (30).

$$\int_0^a \int_0^b \left[\frac{\partial^2 V}{\partial x^2}\frac{\partial^2 w}{\partial x^2} + 2\frac{\partial^2 V}{\partial x \partial y}\frac{\partial^2 w}{\partial x \partial y} + \frac{\partial^2 V}{\partial y^2}\frac{\partial^2 w}{\partial y^2} + KF\frac{\partial^2 V}{\partial y^2}\frac{\partial^2 w}{\partial x^2} \right] dxdy = \lambda^2 MK \int_0^a \int_0^b Vw dxdy \tag{30}$$

Where λ is the eignvalue incorporating the in-plane statically applied normal loads. By substituting for w, F and V from Eqs. (12), (15) and (21) respectively into Eq. (30); and then performing double integrations as required and subsequently solving for eignvalue yields the expression as given in Eq. (31).

$$\lambda^2 = \frac{D}{b^4\beta^4 M}[97.548387 + 236.903226\beta^2 + 504\beta^4 + 1.990215 * 10^{-5}b^4\beta^4 KQA_{12}^2 - 14.806452b^2\beta^4 KP] \quad (31)$$

In order to determine the relation between the fundamental frequency, λ and the axial load *P*, a nondimensional process is carried out. Suppose the axial load *P* is not applied, that is *P = 0*, then the fundamental frequency corresponds to the first mode nonlinear frequency, ω; and Eq. (31) yields Eq. (32).

$$\omega^2 = \frac{D}{b^4\beta^4 M}[97.548387 + 236.903226\beta^2 + 504\beta^4 + 1.990215 * 10^{-5}b^4\beta^4 KQA_{12}^2] \quad (32)$$

However, in the absence of eignvalue (fundamental frequency, λ), the load *P* attains the nonlinear buckling load P_{cr}; and it is expressed as in Eq. (33).

$$P_{cr} = \frac{D}{14.806452b^2\beta^4}[97.548387 + 236.903226\beta^2 + 504\beta^4 + 1.990215 * 10^{-5}b^4\beta^4 KQA_{12}^2] \quad (33)$$

By dividing Eq. (31) by Eq. (32) yields an expression as given in Eq. (34).

$$\left(\frac{\lambda}{\omega}\right)^2 = 1 - \frac{P}{P_{cr}} \quad (34)$$

Or in terms of fundamental frequency:

$$\lambda^2 = \omega^2\left[1 - \frac{P}{P_{cr}}\right] \quad (35)$$

Hence,

$$\lambda = \omega\sqrt{1 - \frac{P}{P_{cr}}} \quad (36)$$

Numerical Experiment and Discussion of Results

Numerical experiments in this work involve the numerical evaluations of the amplitude of deflection at various aspect ratios; the linear and nonlinear fundamental frequencies at various aspect ratios respectively; the linear buckling and nonlinear buckling loads at various aspect ratios respectively. The plate parameters adopted in this study are: E = 10.92MPa, ρ = 100kgm^{-3}, μ = 0.3; a = 1.0m, t = 0.01m, b = open and β = a/b, which were previously used by [33]. These parameters are appropriately substituted into Eqs. (24), (31), (32) and (33) as required. Thus from Eq. 33, the linear buckling load evaluated at aspect ratio equal to one, after deleting the nonlinear terms introduced by the amplitude of deflection, is $5.738\pi^2 Db^{-2}$. When this result is compared with the result found in the previous work in literature [34], the error is 4.90%. Therefore it implies that the technical tool employed in this work is satisfactory.

However, Eq. (36) gives an expression which shows how the ratio of applied compressive load to nonlinear critical load affects the nonlinear fundamental frequency. From Eq. (36), it was observed that there are two bounds (the upper and lower bounds) from which the value of the nonlinear fundamental frequency meaningfully varies. For instance, when the ratio is zero, that is when P = 0, the fundamental frequency attains the value of natural nonlinear fundamental frequency; but when the ratio is equal to unity, then the fundamental frequency attains the value equal to zero, which is the condition that yields the critical buckling load. However, in between these two extreme bounds, the fundamental frequency exhibits decrements or vice versa from or towards a definite bound as represented graphically in Fig. 3. Thus from the given expositions, the design philosophy against dynamic effect or instability needs very careful formulation whenever in-plane statically normal loads are applied.

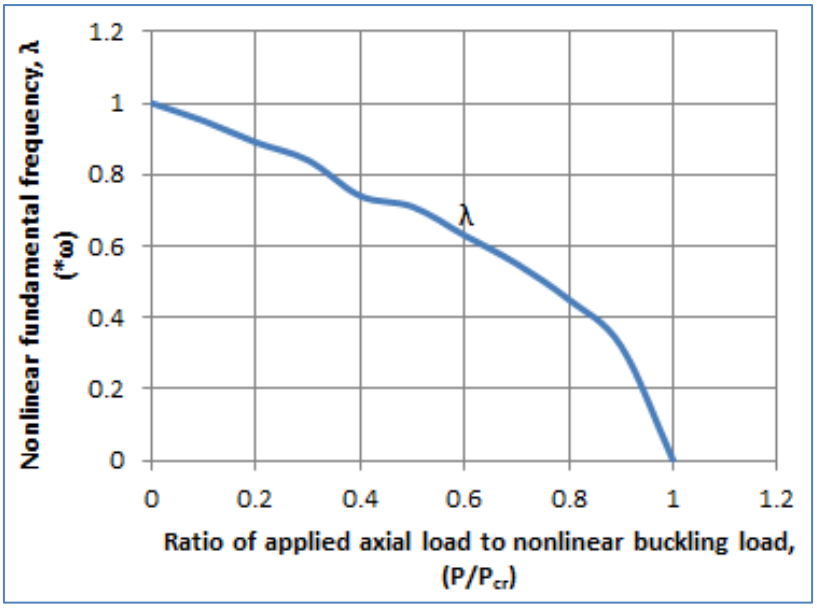

Fig-3: A graphical representation of the variation of nonlinear fundamental frequency with the ratio of applied axial load to nonlinear buckling load

Fig. 4 shows the graphical values of variation of the amplitude of plate deflection with aspect ratios. The amplitude of deflection is the measure of the rigidity characteristics of the rectangular plate. The amplitude of deflection is a strong parameter that influences the nonlinear flexural frequencies of a rectangular plate based on finite deflection.

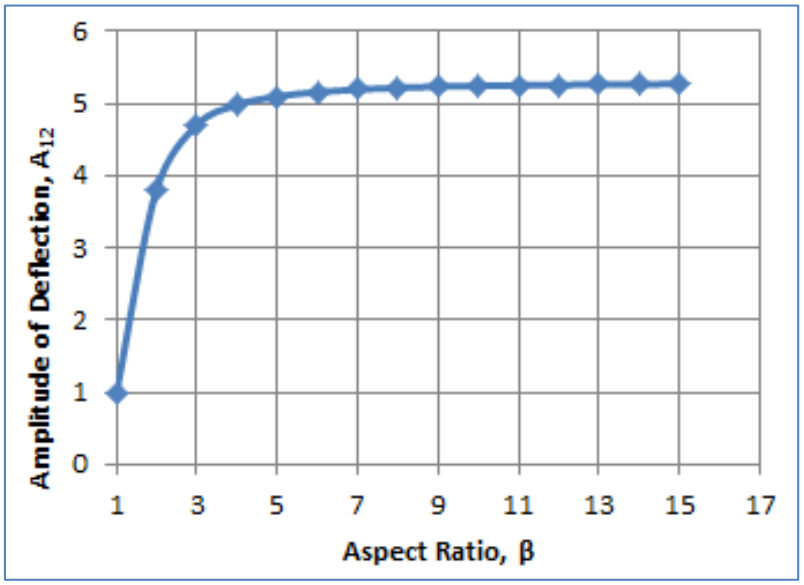

Fig-4: A graphical presentation of amplitude of deflection at various aspect ratios.

From Fig. 4, it was observed that there is a very linearly stiff rise of the graph between the aspect ratio values of one and two; and from aspect ratios two to five, the graph exhibits a parabolic curve. However, from aspect ratio equal to seven to aspect ratio equal to fifteen, the graph exhibits a kind of plateau. Invariably, these graphically curve variations of the amplitude of deflection with aspect ratios are the indications how the nonlinear terms in all the expressions will affect the output.

Fig. 5 presents graphs of the variations of linear and nonlinear fundamental frequencies with aspect ratios. From Fig. 5, it was observed that between the aspect ratios one and two, the difference in the values of linear and nonlinear fundamental frequencies is palely distinct. Furthermore, it was observed from Fig. 5 that there is a very sharp drop in the values of both linear and nonlinear fundamental frequencies from aspect ratio one to aspect ratio two.

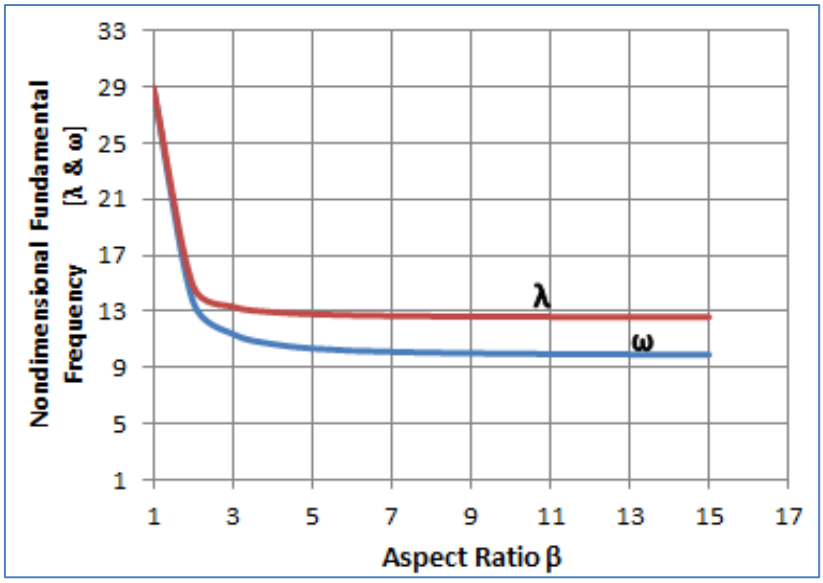

Fig-5: Graphical presentations of linear and nonlinear fundamental frequencies at various aspect ratios

Also, it was observed that above aspect ratio equal to two, the difference in the values of linear and nonlinear fundamental frequencies widens. Moreover, it was observed that from aspect ratio equal to seven and above, the variation of fundamental frequency with aspect ratio becomes almost constant for both of them. Generally, it hereto deduced that the fundamental frequency exhibits soft-spring with aspect ratio. Also, it is deduced that the linear fundamental frequency is numerically equal to nonlinear fundamental frequency at aspect ratio equal to and less than one. Finally, it is deduced that aspect ratio equal to and greater than seven, the variation in fundamental frequency with aspect ratio becomes almost constant.

Fig. 6 presents the graphs of the variations of linear and nonlinear buckling loads with aspect ratios. It was observed that Fig. 6 takes after Fig. 5. Thus from Fig. 6 and Fig. 5, it is here thereafter concluded that there is mapping between eigenvalues and buckling behaviour of the rectangular plate.

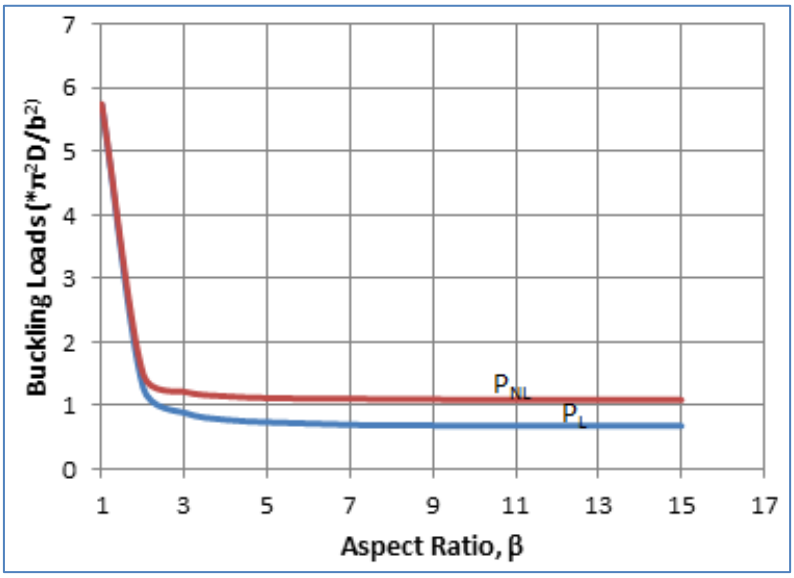

Fig-6: Graphical presentations of linear and nonlinear buckling loads at various aspect ratios

Fig. 7 shows the graphs of the variations in the ratio of nonlinear buckling load to linear buckling load; and the ratio of nonlinear fundamental frequency to linear fundamental frequency with aspect ratios.

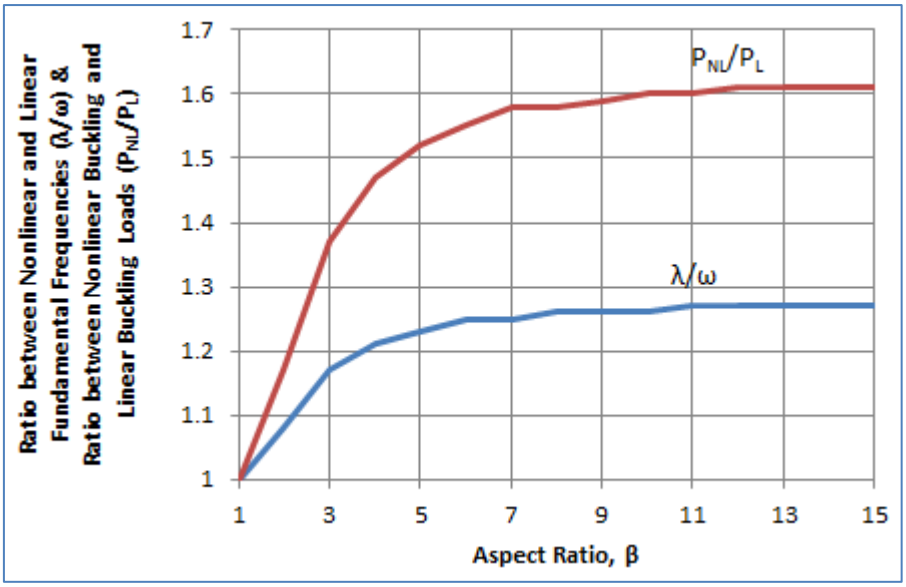

Fig-7: Graphical presentations of ratios between nonlinear and linear buckling loads; and nonlinear and linear fundamental frequencies

From Fig. 7, it was observed that the graphs of the variations in the ratios of nonlinear to linear buckling loads; and of nonlinear to linear fundamental frequencies at aspect ratio equal to and less than three respectively are linear and exhibit hard spring types in their dispositions; and from aspect ratios three to nine, the graphs cease to be linear but become gently curved. However, from aspect ratios nine to fifteen, the graphs exhibit gentle and uniform increases with the tendency to become plateau.

CONCLUSION

This paper determines analytically the effect of in-plane statically applied normal loads on nonlinear fundamental frequency of thin rectangular SCSC plate. The analytical technique used was the weak-form variational method in algebraic polynomial shape functions. From the numerical value of linear buckling load obtained, and in comparison with the results of the previous works found in literature, it is here-in concluded that the weak-form variational principle is a good analytical technique for tackling the problems of stability and dynamic analysis of thin rectangular plates. Furthermore, it is here there-in concluded that the application of algebraic polynomial displacements as shape functions yields satisfactory results. Also, from the analytical and numerical results obtained in this work, it is here-under concluded that statically applied in-plane normal loads have reasonable effect on the nonlinear fundamental frequency of thin rectangular SCSC plates.

REFERENCES

1. Isanaka, B. R., Akbar, M. A., Mishra, B. P., & Kushvaha, V. (2020). Free vibration analysis of thin plates: Bare versus Stiffened. *Engineering Research Express*, *2*(1), 015014.
2. Wu Q, Li L, Zhang YD. Simulations and experiments on vibration control of aerospace thin-walled parts via preload. Shock and Vibration. 2017 Jan 1;2017.
3. Kubiak, T. (2012). Nonlinear plate theory for postbuckling behaviour of thin-walled structures under static and dynamic load. *Nonlinearity, Bifurcation and Chaos: Theory and Applications*, 219.
4. Wang, C. M., Xiang, Y., & Wang, C. Y. (2002). Buckling of standing vertical plates under body forces. *International journal of structural stability and dynamics*, *2*(02), 151-161.
5. Rhodes, J. (2002). Buckling of thin plates and members—and early work on rectangular tubes. *Thin-Walled Structures*, *40*(2), 87-108.
6. Pham, C. H. (2017). Shear buckling of plates and thin-walled channel sections with holes. *Journal of Constructional Steel Research*, *128*, 800-811.
7. da Silva, C. C. C., Helbig, D., Cunha, M. L., dos Santos, E. D., Rocha, L. A. O., de Vasconcellos Real, M., & Isoldi, L. A. (2019). Numerical buckling analysis of thin steel plates with centered hexagonal perforation through constructal design method. *Journal of the Brazilian Society of Mechanical Sciences and Engineering*, *41*(8), 1-18.
8. Van der Neut, A. (1956). *Post buckling behaviour of structures*. ADVISORY GROUP FOR AERONAUTICAL RESEARCH AND DEVELOPMENT PARIS (FRANCE).
9. Watson, A., Kennedy, D., Williams, F. W., & Featherston, C. A. (2003). Buckling and vibration of stiffened panels or single plates with clamped ends. *Advances in Structural Engineering*, *6*(2), 135-144.
10. Dey, P., & Singha, M. K. (2006). Dynamic stability analysis of composite skew plates subjected to

periodic in-plane load. *Thin-walled structures*, *44*(9), 937-942.
11. Ezeh, J. C., Ibearugbulem, M. O., Opara, H. E., & Oguaghamba, O. A. (2014). Galerkin's indirect variational method in elastic stability analysis of all edges clamped thin rectangular flat plates. *International Journal of Research in Engineering and Technology*, *3*(4), 674-679.
12. Reddy, D. R., Ratnam, B. S., & Rao, G. V. (2014). Prediction of dynamic stability behavior of thin square plates subjected to constant compressive and periodic including constant compressive loads on perpendicular edges. *Int. J. Curr. Eng. Technol*, *2*, 620-624.
13. Kowal-Michalska, K., & Mania, R. J. (2008). Some aspects of dynamic buckling of plates under in-plane pulse loading. *Mechanics and Mechanical Engineering*, *12*(2), 135-146.
14. Srivastava, A. K. L., & Pandey, S. R. (2012). Effect of in-plane forces on frequency parameters. *International Journal of Scientific and Research Publications*, *2*(6), 1-18.
15. Zhang, L. W. (2017). On the study of the effect of in-plane forces on the frequency parameters of CNT-reinforced composite skew plates. *Composite Structures*, *160*, 824-837.
16. Carrera, E., Nali, P., Lecca, S., & Soave, M. (2012). Effects of in-plane loading on vibration of composite plates. *Shock and Vibration*, *19*(4), 619-634.
17. Kargarnovin, M. H., & Mamandi, A. (2008). Buckling of generally orthotropic rectangular simply supported edgewise plate under compound in-plane linearly bending-compressive loading, using the Ritz method. In *Proceedings of the 3rd IASME/WSEAS International Conference on Continuum Mechanics, Cambridge, United Kingdom* (pp. 22-29).
18. Tsiatas, G. C., & Yiotis, A. J. (2013). A BEM-based meshless solution to buckling and vibration problems of orthotropicplates. *Engineering Analysis with Boundary Elements*, *37*(3), 579-584.
19. Doiphode, G. S., & Patodi, S. C. (2012). Finding critical buckling load of rectangular plate using integrated force method. *International Journal of Advances in Engineering & Technology*, *5*(1), 288.
20. Kang, J. H., & Leissa, A. W. (2005). Exact solutions for the buckling of rectangular plates having linearly varying in-plane loading on two opposite simply supported edges. *International Journal of Solids and Structures*, *42*(14), 4220-4238.
21. Swamy, M. S., Ranjith, A., Sandya, D. S., & Badami, S. S. (2015). Buckling Analysis of Plate Element Subjected to In Plane Loading Using ANSYS. *Int. Journal of Innovative Research in Science, Engineering and Technology*, *4*(5).
22. Hassan, A. H. A., & Kurgan, N. (2019). Modeling and buckling analysis of rectangular plates in ansys. *International Journal of Engineering and Applied Sciences*, *11*(1), 310-329.
23. Oguaghamba, O. A., Ezeh, J. C., Ibearugbulem, M. O., & Ettu, L. O. (2015). Buckling and Postbuckling Loads Characteristics of All Edges Clamped Thin Rectangular Plate. *The International Journal of Science*, *4*(11), 55-61.
24. Poodeh, F., Farhatnia, F., & Raeesi, M. (2018). Buckling analysis of orthotropic thin rectangular plates subjected to nonlinear in-plane distributed loads using generalized differential quadrature method. *International Journal for Computational Methods in Engineering Science and Mechanics*, *19*(2), 102-116.
25. Beznea, E. F., Vasilache, C. A., & Chirica, I. (2012). FEM buckling behavior studies on composite plates with initial imperfections.
26. Chen, H., & Virgin, L. N. (2006). Finite element analysis of post-buckling dynamics in plates—Part I: An asymptotic approach. *International Journal of Solids and Structures*, *43*(13), 3983-4007.
27. Chuh, M., Narayanaswami, R., & Rao, G. V. (1979). Large amplitude free flexural vibrations of thin plates of arbitrary shape. *Computers & Structures*, *10*(4), 675-681.
28. Rao, G. V., Meera Saheb, K., & Janardhan, G. R. (2008). Simple formula to study the large amplitude free vibrations of beams and plates. *Journal of applied mechanics*, *75*(1).
29. Fung, Y. C. (1965). Foundation of Solid Mechanics. *Prentice Hall, Inc, Englewood Cliff, N. J.*
30. Ventsel, E., Krauthammer, T. (2001). Thin Plates and Shells, Theory, Analysis and Applications, *Marcel Dekker, INC, New York*.
31. Chia, C. Y. (1980). Nonlinear Analysis of Plates. McGraw-Hill International Book Company, USA.
32. Szilard, R. (2004). Theories and Applications of Plate Analysis. *John Wiley and Sons, USA*.
33. Rao, G. V., Raju, I. S., & Raju, K. K. (1976). A finite element formulation for large amplitude flexural vibrations of thin rectangular plates. *Computers & Structures*, *6*(3), 163-167.
34. Ugural, A. C. (2018). Plates and Shells, Theory and Analysis, 4th edition. CRC Press, Taylor and Francis Group.